



KINEMATICS AND DYNAMICS OF SPHERE WAKE TRANSITION

M. C. THOMPSON

*Department of Mechanical Engineering, Monash University
Clayton, VIC 3800, Australia*

T. LEWEKE AND M. PROVANSAL

*Institut de Recherche sur les Phénomènes Hors Equilibre
49, rue Frédéric Joliot-Curie, B.P. 146
F-13384 Marseille Cedex 13, France*

(Received 15 September 2000, and in final form 22 November 2000)

The wake of a sphere undergoes a number of symmetry-breaking transitions as it changes from laminar to turbulent. This paper concentrates on the first two transitions. At $Re = 212$ a *regular* transition occurs, when the wake develops a spectacular *two-tailed* structure consisting of two trailing streamwise vortices. During the second transition at $Re = 272$ the flow undergoes a Hopf bifurcation. In this case there is a complex interaction between the trailing vortices leading to the periodic shedding of vortex loops. Both these transitions are shown to be supercritical (or nonhysteretic). Landau models are constructed for both transitions and the coefficients determined. The visual impression of an apparently sudden bifurcation to the two-tailed wake is shown to be due to the focal nature of the trailing vortices, which draws dye into the cores, even if their net circulation is small. A precursor to the second transition to the periodic wake is strong kinking of the trailing vortices about 1 diameter downstream from the back of the sphere. The vorticity structure of the two-tailed wake prior to transition is also quantified which may prove useful for development of models of the transition process.

© 2001 Academic Press

1. INTRODUCTION

AS THE REYNOLDS NUMBER is increased, the wake behind a sphere undergoes a series of well-defined transitions on its way to becoming fully turbulent. At low Reynolds number the separation bubble is axisymmetric. The attached separation bubble grows in length until the Reynolds number reaches approximately 210.

The first transition involves a (regular) symmetry-breaking topological change from a steady axisymmetric wake with an attached separation bubble to a steady nonaxisymmetric wake consisting of a shortened separation bubble with two trailing counter-rotating vortices. In experimental visualizations dye is trapped in the vortex cores and this leads to a dramatic two-threaded structure shown in Figure 1(a).

Johnson & Patel (1999) found numerically that this transition occurs at approximately $Re_{c_1} = 211$. This value compares well to the value determined by Tomboulides *et al.* (1993) and Tomboulides & Orszag (2000) ($Re = 212$) using a similar numerical formulation to that used to obtain the current results. These values are consistent with experimental predictions which tend to be lower, but have an upper limit close to the numerical estimates. This is

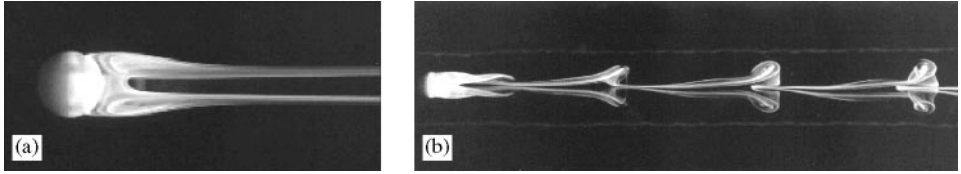


Figure 1. Dye visualizations of the sphere wake: (a) two-tailed stationary wake; (b) wake in the periodic regime.

probably because of perturbations introduced by the support structures. Magarvey & Bishop (1961*a, b*) found the *two-threaded* wake to exist in the range $210 < Re < 270$, Nakamura (1976) found the transition occurred at $Re = 190$, and Ormières (1999) and Ormières & Provansal (1999) observed the two threads between $180 < Re < 280$. In addition, the stability analysis of Natarajan & Acrivos (1993) revealed a *regular*, i.e., time-steady transition at $Re = 210$.

The second topological transition is from the steady two-threaded wake to a periodic wake in which the trailing vortices form kinks that develop into strongly skewed loops, and these move away downstream as shown in Figure 1(b).

Again, there have been various studies documenting and analysing this transition. The critical Reynolds number (Re_{c_2}) has been determined experimentally to be: 280 (Ormières & Provansal 1999), 300 (Sakamoto & Haniu 1995), between 270 and 290 by Magarvey & Bishop (1961*a, b*), and in the range 200–300 in the older study by Taneda (1978). Numerical simulations predict values $Re = 270$ (Johnson & Patel 1999), and in the range 250–280 (Tomboulides *et al.* 1993). In addition, the stability analysis of Natarajan & Acrivos (1993) found the transition to occur at $Re = 277$, although they based the stability analysis on an axisymmetric base flow.

The aim of the present study is to examine certain dynamical and topological features of the first two transitions, in particular, whether they are *subcritical* or *supercritical*, i.e., whether the transitions are hysteretic or not. The initial regular transition, in particular, shows a distinct (apparently discontinuous) change in flow topology and it is difficult to imagine *a priori* how the transition could take place smoothly.

The transitions for the circular cylinder wake are well modelled by the Landau equation; especially in the neighbourhood of the transitions. For example, Dušek *et al.* (1994) apply the model to the transition from steady two-dimensional flow to periodic two-dimensional flow, and Henderson (1997) uses it to describe the transition from two- to three-dimensional shedding. This theory can also be applied to the present system as has been done by Ormières & Provansal (1999), especially for the second transition. They find that the fluctuation energy varies linearly with $(Re - Re_{c_2})$, as expected for a supercritical transition obeying the Landau model.

2. NUMERICAL METHOD

A uniform flow with speed $U_\infty = 1$ was directed along a positive z -axis past a sphere centred at $(z, r, \theta) = (0, 0, 0)$ of radius $R = 1$. The Reynolds number is based on diameter (D) and is defined as $Re = U_\infty D/\nu$, where ν is the kinematic viscosity.

The current simulations employed a spectral/spectral-element method for axisymmetric geometries. A spectral-element discretization was used in the r - z plane and a Galerkin-Fourier expansion in the θ -direction. Typically, sixth-order tensor product Lagrangian polynomial expansions were used in each element and 24 Fourier planes in the θ -direction. An initial study was performed to verify that the resolution was sufficient to resolve the

details of the flow, and selected higher-resolution simulations were used to verify the accuracy of the results. More details about the method can be found in Thompson *et al.* (1996).

3. RESULTS

3.1. THE FIRST TRANSITION

Numerical simulations were performed at Reynolds numbers between 200 and 300. This covers the regular and periodic transitions. Typically, the initial velocity field for the next Reynolds number in the sequence is the asymptotic state of the previous Reynolds number solution examined.

We assume and verify that the initial transition behaves according to the Landau model:

$$\frac{dA}{dt} \approx \sigma A - lA^3, \quad (1)$$

where A represents the (global) perturbation amplitude of some quantity from the base flow. The right-hand side effectively represents the first two terms in a series expansion. The truncation is appropriate in the neighbourhood of the critical Reynolds number providing l is positive, otherwise higher-order terms determine saturation of the unstable mode. The coefficient σ is the growth rate coefficient in the linear regime. It changes from negative to positive through the transition and hence determines the stability of the system. The transition is supercritical if l is positive so that the first nonlinear term causes the initial linear growth of the instability to saturate. If l is negative then the next term in the series is required because that term (or higher-order terms) leads to the saturation of the transient growth. It can be shown (e.g., Dušek *et al.* 1994) that the energy in the mode (A^2) varies as σ/l , which in turn is proportional to $(\text{Re} - \text{Re}_{c_s})$. Thus, the transition can be shown to be supercritical by examining the sign of l and the behaviour of the A^2 away from the transition. (Note that because this transition is from one steady solution to another, A does not need to carry any phase information, so it is sufficient to take it to be real. For the second transition, a Hopf bifurcation, it is necessary to take A and the equation coefficients to be complex numbers.)

Two methods were used to determine the nature of the transition. The first involved recording the time-dependence of the velocity components during the transient evolution at a (mesh) point (4.3, 0, 0) downstream of the sphere. The azimuthal velocity component (w) can be used to monitor the growth of the instability, since it is zero prior to criticality. Although the parameter l may vary in magnitude (because the saturation value of the velocity perturbation will vary from point to point), we expect the sign should be consistent throughout the wake. The linear growth rate (σ) does not vary with position. Since the *amplitude* in the Landau model should be a global property of the wake, another method was used to verify the results obtained by this method. The second method was to define a global amplitude by

$$|A|^2 = \frac{1}{V_{\text{sphere}} U_\infty^2} \int_{\Omega} |(\mathbf{u}_{3D} - \mathbf{u}_{2D})|^2 dV, \quad (2)$$

where the integral is over Ω , the volume of the domain (Henderson 1997). [The nondimensionalization by the volume of the sphere (V_{sphere}) and the upstream speed (U_∞) is arbitrary.] This integral depends on the numerical domain size, which again means that l is not determined uniquely, but since we are mainly interested in the sign of the cubic term this is not a concern.

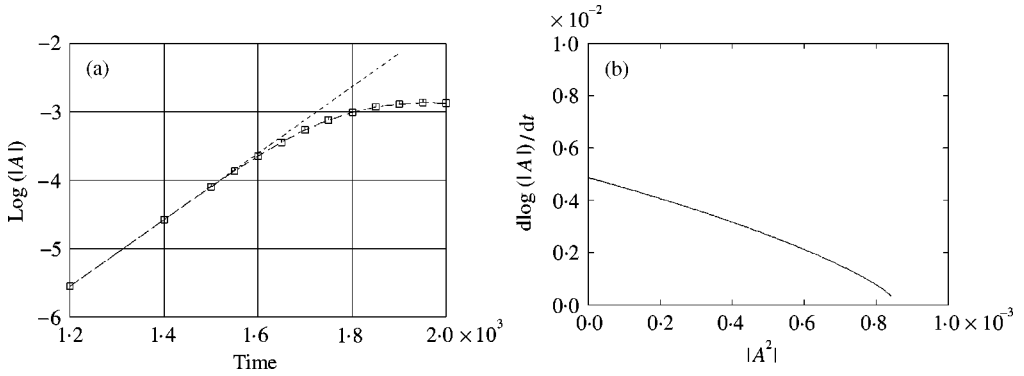


Figure 2. (a) The transition in terms of the global amplitude method. The dashed straight line shows the linear behaviour (for reference). The Reynolds number is 215. (b) Plot of $d \log |A|/dt$ versus $|A|^2$ during transition. The vertical intercept gives the growth rate ($\sigma = 0.004868$) and the gradient is equal to $l (= 3.78)$. The linear behaviour near $|A|^2 = 0$ also verifies that the first nonlinear term in the Landau model is a cubic term. The deviation from linearity for higher values indicates that higher-order terms become important close to saturation.

One determination of the critical Reynolds number is obtained from the behaviour of the linear growth rate (σ) versus Reynolds number. Using a quadratic fit to the growth rate measured at $Re = 205, 215,$ and 220 , it becomes positive at $Re_{c_1} = 212$, close to predictions from other direct simulations and stability analysis.

The nature of the transition was determined by the sign of l for $Re = 215$; just slightly in excess of the critical Reynolds number. Figure 2(a) shows the logarithm of the amplitude of global perturbation mode. The evolution using the point method (not shown) is consistent with this behaviour. This graph indicates the supercritical nature of the transition since the initial deviation from linearity is to decrease the growth rate.

The parameters σ and l can be determined accurately by plotting $d \log |A|/dt$ versus $|A|^2$. For the point speed method this plot is shown in Figure 2(b). The y-intercept corresponds to σ , and the gradient gives l . The values are $\sigma = 0.004868$ and $l = 3.78$. This growth rate agrees with the value obtained by the global mode method.

Note that the Landau model theory (and dimensional analysis) suggests that the growth rate depends on the diffusion timescale and the distance to the critical Reynolds number, i.e.,

$$\frac{1}{\sigma} \sim \frac{D^2}{\nu} (Re - Re_{c_1})^{-1}. \tag{3}$$

For $Re = 215$, the right-hand side is 129, given $(Re - Re_{c_1}) \approx 3$, while the actual growth rate timescale is $1/0.00486 = 205$.

The Landau model also predicts that the square of the amplitude of the perturbation should be proportional to $(Re - Re_{c_1})$ close to the transition. Figure 3 shows the behaviour of the energy in the saturated mode as a function of Reynolds number. A convenient measure of the energy is given by the azimuthal component, i.e.,

$$|A_\theta|^2 = \frac{1}{V_{\text{sphere}} U_\infty^2} \int_{\Omega} |w|^2 dV. \tag{4}$$

This is used because it does not require the calculation of the two-dimensional base flow (since the azimuthal velocity component is zero prior to transition).

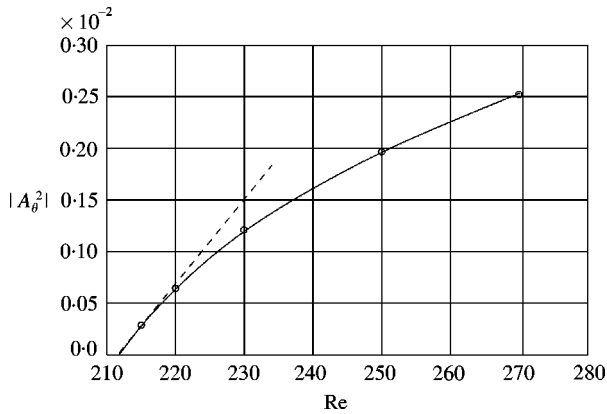


Figure 3. Plot of $|A_0|^2$ against Reynolds number again confirming the transition is supercritical and well described by the Landau model.

3.2. THE TRANSITION PROCESS

There has been some discussion in the literature of the physical process leading to the transition and maintenance of the saturated state. For example, Johnson & Patel (1999) examine the process in terms of pressure, and Shirayama (1992) in terms of limiting surface streamlines. Some insight into the physical mechanism behind the bifurcation can be gained by examining the development of streamwise vorticity during the transition. Figure 4(a) shows streamwise vorticity isosurfaces corresponding to $\omega_z = \pm 0.01$ at time 1400. Again the Reynolds number is 215. This is still in the linear growth regime. The initial development of streamwise vorticity apparently results from the tilting of azimuthal vorticity generated on the surface of the sphere. Below the transition point, rings of fluid which pass close to the surface of the sphere maintain their axes pointing along the z -axis. Above the critical point these rings become tilted, as can be verified by examining isosurfaces of stream-wise velocity component near the surface of the sphere. This tilting converts the azimuthal vorticity into streamwise vorticity — positive on one side of the sphere and negative on the opposite side, as is shown in Figure 4(a). After generation, the vorticity is carried away from the surface into the wake flow when the flow separates from the separation line at the back of the sphere. This process produces the double-threaded wake structure as seen in the experiments. The threads maintain considerable vorticity downstream as shown in Figure 4(b), which displays the wake structure at saturation. Johnson & Patel (1999) discuss the transition process in more detail and in particular demonstrate that the transition from axial to planar symmetry is associated with the out-of-symmetry-plane velocity component in the wake.

As commented previously, the experiments indicate that the two-threaded wake seems to appear quite suddenly once the critical Reynolds number is exceeded. Also note the apparently discontinuous change in wake topology, which seems to suggest that the transition might be subcritical. However, it is difficult for experiments to determine hysteresis directly. As shown in the previous section, the Landau model indicates the transition is not subcritical. The visualization of the developing streamwise vortex filaments shown in Figure 4(a) provide an explanation of why the dye filaments appear to occur discontinuously at transition. The visualization shows that there is a release of streamwise vorticity into the wake from distinct points on opposite sides of the attached separation

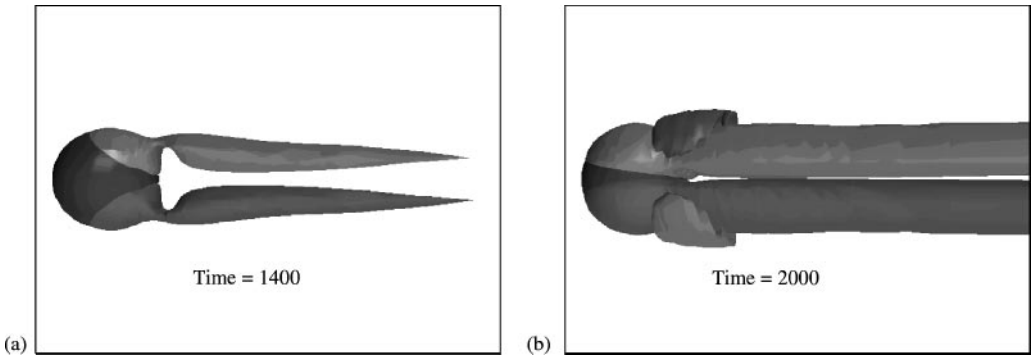


Figure 4. (a) Isosurfaces of positive and negative streamwise vorticity ($\omega_z = \pm 0.01$) in the neighbourhood of the sphere during the transition to non-axisymmetric flow for $Re = 215$. (b) Isosurfaces at saturation for the same Reynolds number.

bubble. Note that this visualization shows the *shape* of linear instability mode structure. Importantly, the two trailing vortices do not migrate from the centreline as they grow in strength. Even very close to transition, although these structures possess little streamwise vorticity, they act as stable foci and hence draw dye into their cores. Thus, it is expected that there should be a sudden change to the wake at transition as monitored by dye visualizations.

3.3. WAKE DEVELOPMENT AFTER THE FIRST TRANSITION

The wake in this regime is characterized by counter-rotating vortex threads, usually observed in the experiments as two trailing dyelines. The counter-rotating vortices induce a velocity at the centreline of each other causing them to be convected away from the centreplane.

For $Re = 250$, the vortex thread structures are visualized in Figure 5. This figure shows a top and side view of the threads highlighted by plotting the 0.015-isosurface of the imaginary component of the eigenvalue of the velocity gradient tensor [e.g., Mittal (1999)].

The diffusion timescale $D^2/\nu = Re D/U_\infty$ is approximately 500 for the dimensions used in the current simulations. Since the velocity in the wake is approximately the free-stream velocity, this means that diffusion is slow to cross-diffuse the two vortex threads, so they should preserve some strength for a considerable distance downstream even though they are close together.

Cross-sectional contour plots of the streamwise vorticity are shown in Figure 6 at $z = 3R$ and $12R$ downstream of the sphere. The contours deviate considerably from circularity even in the cores, presumably due to both cross-diffusion and the initial formation mechanism. Concerning the latter, Johnson & Patel (1999) have demonstrated that the tilting of vortex rings (as discussed above) in the initial formation region leads to streamwise vorticity being shed from a more downstream portion of the recirculation region. However, it is still possible to fit the profiles reasonably well using a combination of Gaussian vorticity distributions.

A least-squares fit of the actual vorticity distribution was computed for the following functional fit:

$$\begin{aligned} \bar{\omega}_z = & -S \exp[-(x - x_0)^2/a^2 - (y - y_0)^2/b^2] \\ & + S \exp[-(x + x_0)^2/a^2 - (y - y_0)^2/b^2] \end{aligned} \quad (5)$$

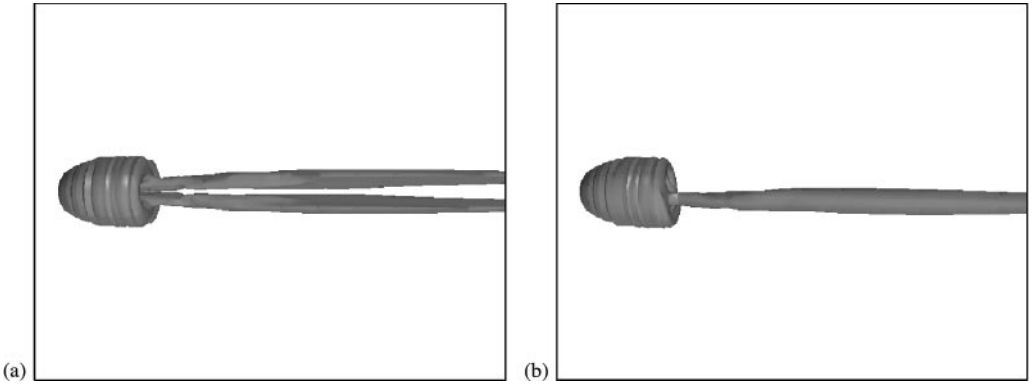


Figure 5. (a) Top and (b) side view of the trailing vortex threads for $Re = 250$. See text for details. The view of the sphere is obstructed by the isosurface. Note the irregularity of the structure covering the sphere is an artefact of the nonregular node-point distribution.

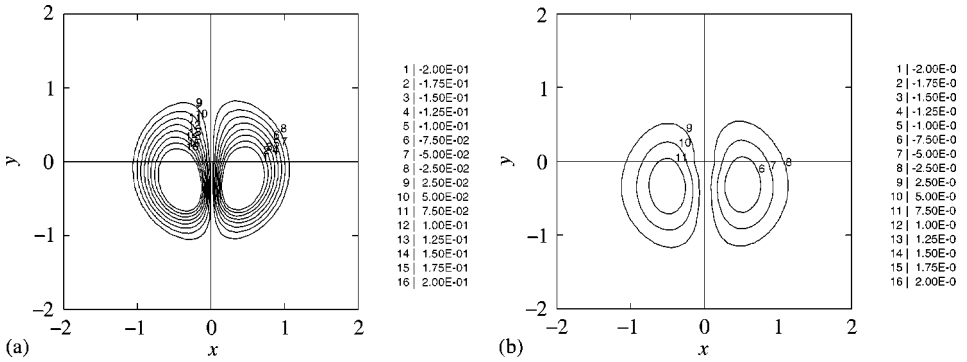


Figure 6. Streamwise vorticity contours for $Re = 250$ at (a) $z = 3R$ and (b) $12R$.

with z in the range $[2R, 15R]$. Here x and y are the Cartesian coordinates in the cross-planes. There are five fitting parameters: S , a , b , x_0 and y_0 . The goodness of fit improves further downstream. A typical indication of the fit is shown in Figure 7 for $Re = 250$ and $z = 10R$. Notice that the distribution in the y -direction is not symmetrical about the centre of each vortex; this is probably at least partially due to the induced velocity moving the vortices away from the centreplane.

The variation of the parameters as a function of distance and Reynolds number is shown in Figure 8. Interestingly, these figures show increased kinking of the trailing vortex filaments at 3 radii downstream from the sphere centre as the Reynolds number gets close to Re_{c_2} , especially noticeable in terms of the distance parameter x_0 . The tails get closer together at this point, before moving apart again. Figure 9 is an isosurface plot of the tail structure at $Re = 270$, only slightly below the transition Reynolds number Re_{c_2} . This clearly shows the distortion. The kinking is considerably weaker at lower Reynolds numbers such as shown in Figure 5. It seems reasonable to speculate that this may be associated with the transition to the periodic wake. A typical post-transition visualization of the tail structure is shown in Figure 9(b) (see also Mittal 1999).

Figure 8(f) shows the variation of maximum vorticity in the threads as a function of downstream distance for $Re = 250$. This indicates the vorticity at the centre of the threads

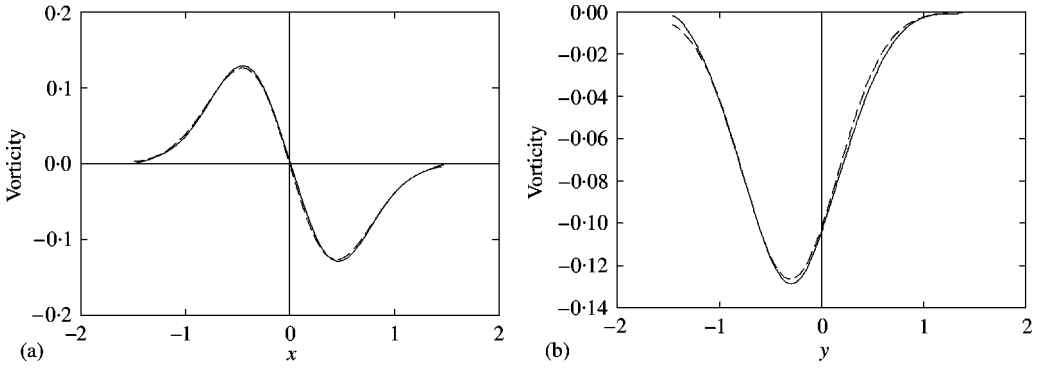


Figure 7. Variation of streamwise vorticity through the centres of the vortices in (a) the x -direction and (b) the y -direction. Solid lines show numerical predictions and dashed lines are least-squares fits; $Re = 250, z = 10R$.

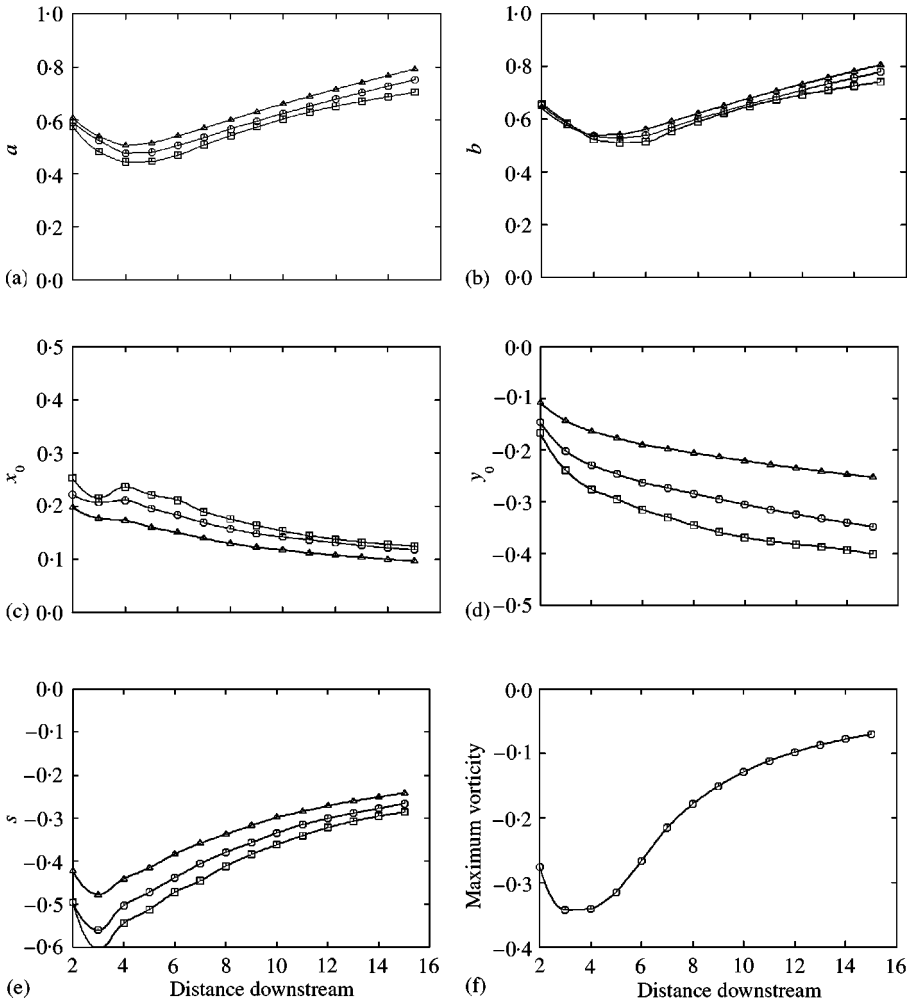


Figure 8. Size parameters (a) a and (b) b , position parameters (c) x_0 and (d) y_0 , and (e) strength parameter S : Δ , $Re = 230$; \circ , $Re = 250$; \square : $Re = 270$. (f) Variation of maximum vorticity in the trailing vortex threads with downstream distance.

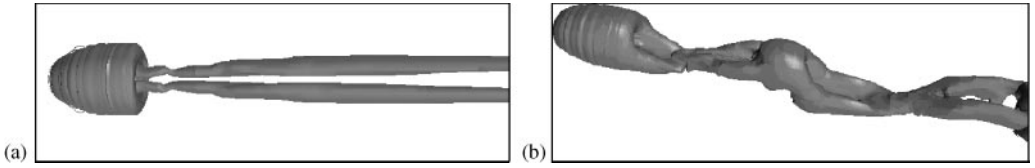


Figure 9. Isosurface plot of the vorticity structure. (a) Two-tailed wake at $Re = 270$, just below the transition to periodic wake flow. (b) $Re = 290$ (side view).

decays (through diffusion and cross-annihilation) by a factor of about three over the first five diameters downstream of the sphere. The decay is much slower further down, and clearly the vortices maintain some strength for a considerable distance downstream.

3.4. THE SECOND TRANSITION

According to the current simulations, between $Re = 270$ and 280 the transition from a stationary nonaxisymmetric wake to a periodic nonaxisymmetric wake takes place.

At $Re = 270$ the growth rate for the development of the periodic mode is $a_R = -0.00283$, while at $Re = 280$ the value is $a_R = 0.015$. Linear interpolation between these two values indicates that the transition occurs at about $Re_{c_2} \approx 272$. This is consistent with other numerical predictions described previously [e.g., Johnson & Patel (1999), Tomboulides *et al.* (1993), Tomboulides & Orszag (2000)] and slightly lower than the transition value of 277 predicted by the linear stability analysis of Natarajan & Acrivos (1993).

In this case, because phase information is required, the transition is modelled by the complex Landau equation

$$\frac{dA}{dt} = (a_R + ia_I)A - l_R(1 + ic)|A|^2A. \quad (6)$$

By assuming a solution of the form $A = \rho \exp[i\phi(t)]$, this complex equation can be decomposed into an equation for the amplitude, ρ , and an equation for the phase, $\phi(t)$. The equation for the (real) amplitude is of the same form as before

$$\frac{d\rho}{dt} = a_R\rho - l_R\rho^3 \quad (7)$$

[see Le Gal *et al.* (2001), this issue, for more details]. As for the previous transition, the nature of the instability can be assessed by examining the sign of the (real) Landau coefficient (l_R). Figure 10(a) shows the growth and saturation of the periodic wake. Initially, the flow receives a large jolt as the Reynolds number is increased from $Re = 270$ to 280 . The transient dies away while the growth of the instability is still in the linear regime.

Numerical estimates of the coefficients in the Landau model can be obtained from Figure 10(b) which shows the variation of $d \log|V_{amp}|/dt$ with $|V_{amp}|^2$, where $|V_{amp}|$ is the amplitude of the velocity in the $r-\theta$ plane at the sampling point $(4.3, 0, 0)$. This plot provides values of $a_R = 0.015$ and $l_R = 40.54$, verifying the transition is supercritical. This finding is consistent with the experimental investigations of Ormières & Provansal (1999) who demonstrated supercriticality by showing the linear variation of perturbation energy with Reynolds number above the transition value. An attempt is currently being made to verify the conclusion of the point method by using the global amplitude method. The results will be reported elsewhere.

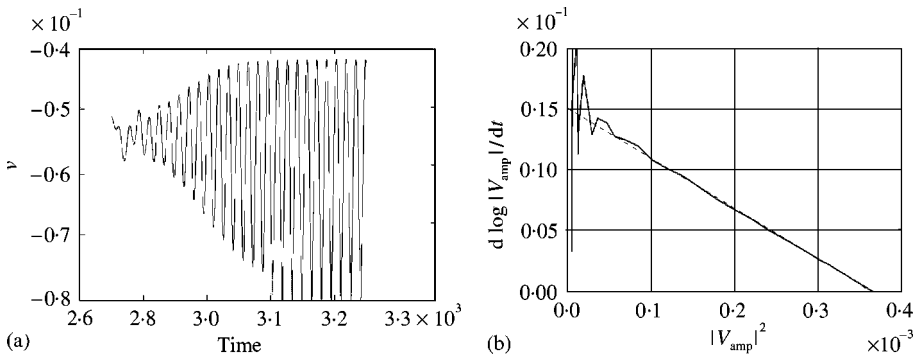


Figure 10. (a) Growth and saturation of the wake instability at $Re = 280$ as measured by the vertical velocity component at a point in the wake. (b) $d \log |V_{amp}| / dt$ versus $|V_{amp}|^2$ used to determine the values of a_R and l_R . This indicates the transition is supercritical.

Simulations closer to the transition Reynolds number have also allowed an accurate determination of the Landau constant of $c = -0.554$ at $Re = 273$. It is of interest that this is significantly smaller in magnitude than the corresponding value $c \simeq -3$ for the Hopf bifurcation for a circular cylinder wake [e.g., Dušek *et al.* (1994), Le Gal *et al.* (2001)].

4. CONCLUSIONS

This paper has examined the first two transitions in the wake of a sphere. Both the regular transition at $Re = 212$ and the Hopf bifurcation at $Re = 272$ are supercritical (or nonhysteretic), as determined from the evaluation of the cubic coefficients of the Landau model. The apparent sudden occurrence of the two-threaded wake structure observed in the experiments seems to be due to the release of streamwise vorticity into the wake from distinct points on opposite sides of the attached separation bubble. Even though these stream wise vortical structures possess little vorticity close to the transition Reynolds number, they act as stable foci and hence draw dye into their cores, leading to the possible misinterpretation of the transition as subcritical.

The vortical structure of the trailing threads has also been quantified and clearly shows kinking at about 3 radii downstream of the centre as the Reynolds number approaches the critical value. It may be possible to use this quantitative description of the wake to construct a simplified physical model of the transition process.

REFERENCES

- DUŠEK, J., LE GAL, P. & FRAUNIÉ, P. 1994 A numerical and theoretical study of the first Hopf bifurcation in a cylinder wake. *Journal of Fluid Mechanics* **264**, 59–80.
- HENDERSON, R. D. 1997 Nonlinear dynamics and pattern formation in turbulent wake transition. *Journal of Fluid Mechanics* **352**, 65–112.
- JOHNSON, T. A. & PATEL, V. C. 1999 Flow past a sphere up to a Reynolds number of 300. *Journal of Fluid Mechanics* **378**, 19–70.
- LE GAL, P., NADIM, A. & THOMPSON, M. 2001 Hysteresis in the forced Stuart–Landau equation: application to vortex shedding from an oscillating cylinder. *Journal of Fluids and Structures* **15**, 445–457.
- MAGARVEY, R. H. & BISHOP, R. L. 1961a Transition ranges for three-dimensional wakes. *Canadian Journal of Physics* **39**, 1418–1422.
- MAGARVEY, R. H. & BISHOP, R. L. 1961b Wakes in liquid–liquid systems. *Physics of Fluids* **4**, 800–805.
- MITTAL, R. 1999 Planar symmetry in the unsteady wake of a sphere. *AIAA Journal* **37**, 388–390.

- NAKAMURA, I. 1976 Steady wake behind a sphere. *Physics of Fluids* **19**, 1–18.
- NATARAJAN, R. & ACRIVOS, A. 1993 The instability of the steady flow past spheres and disks. *Journal of Fluid Mechanics* **254**, 323–344.
- ORMIÈRES, D. 1999 Etude expérimentale et modélisation du sillage d'une sphère à bas nombre de Reynolds. Ph.D. Dissertation, Université de Provence, Marseille, France.
- ORMIÈRES, D. & PROVANSAL, M. 1999 Transition to turbulence in the wake of a sphere. *Physical Review Letters* **83**, 80–83.
- SAKAMOTO, H. & HANIU, H. 1995 The formation mechanism and shedding frequency of vortices from a sphere in a uniform shear flow. *Journal of Fluid Mechanics* **287**, 151–171.
- SHIRAYAMA, S. 1992 Flow past a sphere: topological transitions in the vorticity field. *AIAA Journal* **30**, 349–358.
- TANEDA, S. 1978 Visual observations of the flow past a sphere at Reynolds numbers between 10^4 and 10^6 . *Journal of Fluid Mechanics* **85**, 187–192.
- THOMPSON, M. C., HOURIGAN, K. & SHERIDAN, J. 1996 Three-dimensional instabilities in the wake of a circular cylinder. *Experimental Thermal and Fluid Science* **12**, 190–196.
- TOMBOULIDES, A. G. & ORSZAG, S. A. 2000 Numerical investigation of transitional and weak turbulent flow past a sphere. *Journal of Fluid Mechanics* **416**, 45–73.
- TOMBOULIDES, A. G., ORSZAG, S. A. & KARNIADAKIS, G. E. 1993 Direct and large eddy simulations of axisymmetric wakes. AIAA Paper 93-0546.
- WILLIAMSON, C. H. K. 1988 The existence of two stages in the transition to three-dimensionality of a cylinder wake. *Physics of Fluids* **31**, 3165–3168.